Since January 2020 Elsevier has created a COVID-19 resource centre with free information in English and Mandarin on the novel coronavirus COVID-19. The COVID-19 resource centre is hosted on Elsevier Connect, the company's public news and information website.

VIROLOGY 230, 93–102 (1997)
ARTICLE NO. VY978460

Recombinant Genomic RNA of Coronavirus MHV-A59 after Coreplication with a DI RNA Containing the MHV-RI Spike Gene

LINONG ZHANG,*,†,[1] FELIX HOMBERGER,† WILLY SPAAN,* and WILLEM LUYTJES*,[2]

Department of Virology, Leiden University, Leiden, The Netherlands; and †Institute of Laboratory Animal Science, University of Zurich, Zurich, Switzerland

Received November 21, 1996; returned to author for revision January 6, 1997; accepted January 23, 1997

A strategy for targeted RNA recombination between the spike gene on the genomic RNA of MHV-A59 and a synthetic DI RNA containing the MHV-RI spike gene is described. The MHV-RI spike gene contains several nucleotide differences from the MHV-A59 spike gene that could be used as genetic markers, including a stretch of 156 additional nucleotides starting at nucleotide 1497. The MHV-RI S gene cDNA (from nucleotide 277-termination codon) was inserted in frame into pMIDI, a full-length cDNA clone of an MHV-A59 DI, yielding pDPRIS. Using the vaccinia vTF7.3 system, RNA was transcribed from pDPRIS upon transfection into MHV-A59-infected L cells. DPRIS RNA was shown to be replicated and passaged efficiently. MHV-A59 and the DPRIS DI particle were copassaged several times. Using a highly specific and sensitive RT-PCR, recombinant genomic RNA was detected in intracellular RNA from total lysates of pDPRIS-transfected and MHV-A59-infected cells and among genomic RNA that was agarose gel-purified from these lysates. More significantly, specific PCR products were found in virion RNA from progeny virus. PCR products were absent in control mixes of intracellular RNA from MHV-A59-infected cells and *in vitro*-transcribed DPRIS RNA. PCR products from intracellular RNA and virion RNA were cloned and 11 independent clones were sequenced. Crossovers between A59 and RI RNA were found upstream of nucleotide 1497 and had occurred between 106 nucleotides from the 5′-border and 73 nucleotides from the 3′-border of sequence homologous between A59 and RI S genes. We conclude that homologous RNA recombination took place between the genomic RNA template and the synthetic DI RNA template at different locations, generating a series of MHV recombinant genomes with chimeric S genes.

INTRODUCTION

Coronaviruses are a group of enveloped viruses containing a single-stranded, positive sense RNA genome of approximately 27–32 kb in length. Mouse hepatitis virus (MHV), one member of the coronavirus group, is highly contagious in laboratory mouse colonies and causes a wide spectrum of disease manifestations ranging from subclinical infections to high mortality. MHV strains can be divided, based on their sites of initial replication, into two biotypes: respiratory (polytropic) and enterotropic. After orinasal inoculation, respiratory strains like MHV-A59 will replicate initially in the mucosa of the upper respiratory tract and then, depending on the susceptibility of the mouse, disseminate to multiple organs like liver or brain but not to the intestine. In contrast, the enterotropic strains such as MHV-Y and MHV-RI are largely restricted to the intestinal mucosa, the site of their primary replication, with minimal dissemination to other organs (Barthold, 1986, 1987; Barthold *et al.,* 1993; Compton *et al.,* 1993).

The MHV virion consists of four to five structural proteins: the spike protein (S), the membrane protein (M), the small membrane protein (E), and the nucleocapsid protein (N). An additional protein, the hemagglutinin esterase (HE), is found in some strains. The S protein forms the characteristic peplomer on the virion surface and is responsible for virus binding to cell receptor, induction of cell-to-cell fusion, elicitation of neutralizing antibodies, and cell-mediated immunity (Collins *et al.,* 1982; Daniel and Talbot, 1990; Hasony and Macnaughton, 1981). Although the molecular mechanism of the MHV tissue tropism is still poorly understood, several studies have shown an important role of the S protein in determining the viral virulence and pathogenesis (Dalziel *et al.,* 1986; Fazakerley *et al.,* 1992; Fleming *et al.,* 1986; Hingley *et al.,* 1994; Wege *et al.,* 1988).

One way to study the molecular basis of coronavirus tissue tropism determination is to insert candidate tropism genes, particularly the S gene, from an enterotropic MHV strain into a respiratory strain and study the tropism of the resulting virus. This would require an infectious cDNA clone which, due to the size of the MHV genome, is as yet technically impossible to generate. However, an alternative may lie in the application of RNA recombination. MHV strains have been shown to undergo *in vitro* and *in vivo* homologous recombination at a very high frequency (Lai *et al.,* 1985; Makino *et al.,* 1986, 1987; Keck

[1] Present address: Department of Biology, McMaster University, 1280 Main Street West, Hamilton, Ontario, Canada L8S 4K1.

[2] To whom correspondence and reprint requests should be addressed. E-mail: Luytjes@virology.azl.nl.

0042-6822/97 $25.00

et al., 1987, 1988) and it is believed that recombination is an important feature of coronavirus evolution. Interestingly, RNA recombination also occurs between coronavirus genomic RNA and synthetic RNAs, in particular transcripts from cDNA copies of defective interfering (DI) RNAs (Koetzner *et al.,* 1992; Van der Most *et al.,* 1992). These DI RNAs, truncated genomes that have retained the replication signals but are dependent on helper virus to provide the necessary proteins for replication, can be mutagenized as long as replication signals are not affected (Van der Most *et al.,* 1991; Luytjes *et al.,* 1996). There are several reports on the successful introduction of mutations into the 3′- and 5′- terminal regions of the MHV genome by using recombination with synthetic DI RNAs (Koetzner *et al.,* 1992; Van der Most *et al.,* 1992; Masters *et al.,* 1994; Peng *et al.,* 1995). However, this approach does not allow mutagenesis of the internally located genes. In this paper we report the use of RNA recombination to generate chimeric S genes in the respiratory coronavirus MHV-A59 genome, by making use of a coreplicating synthetic DI RNA containing the enteric coronavirus MHV-RI S gene. This will be an important step toward isolating recombinant viruses.

MATERIALS AND METHODS

Cells and viruses

Mouse L cells (Spaan *et al.,* 1981) were grown in Dulbecco's modified Eagles medium (DMEM) containing 10% fetal calf serum (FCS). MHV-A59 was grown in 17CL-1 cells to prepare high-titered virus stocks. MHV-RI was originally isolated in CMT-93 cells from an infected nude mouse intestine and was passaged either in infant mice or in J774A.1 cells (Barthold *et al.,* 1985). J774A.1 cells were obtained from the American Type Culture Collection (Rockville, MD) and maintained in RPMI medium 1640 supplemented with 10% FCS. L cells were used for infection and transfection experiments. Stocks of recombinant vaccinia virus vTF7.3 (Provided by Bernard Moss, NIH) were prepared in rabbit kidney cells (RK 13).

MHV-RI S gene cDNA synthesis and cloning

Briefly, mouse intestinal homogenates were diluted in TNE buffer (50 m*M* Tris–HCl, pH 7.5, 100 m*M* NaCl, 1 m*M* EDTA) with RNasin, extracted by SDS/proteinase K treatment, phenol-chloroform extraction, and ethanol precipitation. Reverse transcription was done by using avian myeloblastosis virus (AMV) reverse transcriptase (Promega, Madison, WI) followed by PCR amplification with Taq polymerase (Boehringer Mannheim, Mannheim, Germany). First strand cDNA was synthesized using primers LTK8 and LTK52 (Table 1), respectively. Two overlapping PCR fragments were generated using two sets of primers LTK8-LTK51 (Table 1) and LTK52-LTK53 (Table 1). PCR products were cloned into the *Sma*I site of pUC-18 by T4 DNA ligase using a cloning kit (Pharmacia, Uppsala, Sweden). The resulting clones LTK8-51 and LTK52-53, in which the overlapping region contained a unique *Cla*I site, were digested with *Cla*I and *Kpn*I. The smaller fragment from clone LTK8-LTK51 and larger fragment from clone LTK52-LTK53 were isolated from low melting point agarose gel and ligated together, yielding a full-length MHV-RI S gene cDNA clone, pMHVRIS.

Construction of pDPRIS

The construction of pDPRIS was performed in several steps. To shorten the length of the DI vector, the *Mlu*I and *Nhe*I fragment of the MIDI-derivative pMIDI-ΔPst (Van der Most *et al.,* 1995) was replaced by the corresponding fragment of another MIDI derivative pDIF-85T (Van der Most *et al.,* 1995), which resulted in pMIDI-ΔPst*. A linker containing *Bgl*II and *Kpn*I sites was introduced into the unique *Hin*dIII site of pMIDI-ΔPst*. A *Bam*HI linker was inserted into the unique *Pme*I site of pMHVRIS. *Bam*HI and *Kpn*I were used to digest the RI S gene from pMHVRIS as a 3.9-kb fragment, stretching from nt 277 into the downstream MHV-RI ORF4 sequence. This fragment was ligated into *Bgl*II- and *Kpn*I-digested pMIDI-ΔPst*, resulting in two independently isolated clones pDPRIS-4YL and -1L, in which the RI S gene was fused in frame with ORF 1a of pMIDI-ΔPst*.

In vitro transcription and translation

pDPRIS was linearized with *Nhe*I and subjected to *in vitro* transcription using T7 RNA polymerase as described (Van der Most *et al.,* 1991). *In vitro* translation was done in a 10-μl reaction mixture containing nuclease-treated, methionine-depleted rabbit reticulocyte lysate (Promega), supplemented with 10 μCi ^{35}S-labeled methionine (>1000 Ci/mmol, Amersham), 20 m*M* unlabeled amino acids mixture lacking methionine (Promega), and 10–50 ng of *in vitro*-transcribed RNA. The labeled proteins were directly analyzed by electrophoresis in sodium dodecyl sulfate (SDS)–12.5% polyacrylamide gels (PAGE) and autoradiography.

DNA transfection and *in vivo* transcription

Confluent L cells grown in 35-mm wells were infected at a multiplicity of infection (m.o.i.) of 5 with the recombinant vaccinia virus vTF7.3 which encodes the T7 polymerase. One hour after infection the supernatant containing the vaccinia virus was removed and the cells were transfected with 1 μg pDPRIS. The transfection mixture was prepared as follows: 10 μl lipofectin (BRL, Gaithersburg, MD) was diluted in 200 μl DMEM without FCS, mixed with 1 μg of pDPRIS DNA, and incubated at room temperature for 10 min, then 800 μl of DMEM without FCS was added. Three and a half hours posttransfection the cells were infected with MHV-A59 at a m.o.i. of 10.

Virus progeny was harvested after 8 hr incubation at 37°. This virus progeny is defined as passage 0 (P0).

Isolation and analysis of viral RNAs

MHV-A59 and DPRIS DI particles were copassaged several times in cell culture. To isolate intracellular RNA, cells were lysed directly in wells by adding 1 ml of Trizol reagent (Total RNA isolation reagent, BRL) to 3.5-cm-diameter wells and the lysate was suspended. Then RNA was isolated according to the manufacturer's instructions. For the isolation of RNA from purified virions, labeled virus particles were obtained by adding at 4 hr p.i. a mixture of 1 ml DMEM lacking methionine and cysteine and 20 μl [^{35}S]methionine. Supernatants from coinfected cell cultures were harvested 4 hr later (8 hr p.i.), layered onto a discontinuous 20–50% sucrose gradient and centrifuged for 16 hr at 35,000 g. Subsequently 18 fractions of 500 μl were collected. Five microliters of each fraction was spotted on Whatman paper and TCA-precipitated. After counting the samples in a scintillation counter, three peak fractions were combined and the volume was adjusted to 5 ml with TESV (20 m*M* Tris, pH 7.4, 1 m*M* EDTA, pH 8.0, 100 m*M* NaCl). The virions were collected and pelleted again by centrifugation at 120,000 *g* for 4 hr. Purified virions were treated with proteinase K (1 μg/ml) and 0.5% sodium dodecyl sulfate (SDS) and virion genomic RNA was isolated as described (Spaan *et al.,* 1981). To purify MHV genomic RNA from DI RNA, intracellular RNA was separated on a formaldehyde-1% low melting point agarose gel by electrophoresis. Duplicate RNA samples were loaded and half the gel was used to locate the genomic RNA by hybridization. The genome size RNA band was excised from the corresponding area of the other half of the gel and melted for 5 min at 70°. Twenty milligrams of yeast tRNA (type x, Sigma) was added to each sample and then RNA was eluted from the gel as described previously (Langridge *et al.,* 1980; Makino *et al.,* 1984). For hybridization, RNA samples were separated in formaldehyde-agarose gels (Sambrook *et al.,* 1989). The gels were dried and hybridized with 5′-end-labeled oligonucleotide probes (Meinkoth and Wahl, 1984). Oligonucleotides were labelled with (r-^{32}P-labeled dATP) and T4 polynucleotide kinase.

Reverse transcription and PCR amplification (RT-PCR)

The oligonucleotides used for this study are listed in Table 1. Three specific RT-PCRs were developed for the detection of DPRIS, MHV-A59, and recombinants. Reverse transcription was done using AMV reverse transcriptase (Promega) followed by PCR amplification with Taq polymerase (Boehringer Mannheim). PCR was performed for 35 cycles, each consisting of 1 min at 94°, 1 min at 49° and 2 min at 72°. For the detection of DPRIS, first-strand cDNA synthesis was carried out with primer C147, followed by PCR amplification using primer pair C30 and C147. C147 is located in the RI spike gene in an area deleted in MHV-A59. C30 binds to a sequence within ORF1a of MHV-A59 gene 1, which lies immediately upstream of the RI S gene in DPRIS. This primer pair for RT-PCR will generate a positive signal only when DPRIS is present. To detect the MHV-A59, C142 was used to prime cDNA synthesis. This primer is located at the 5′ end of MHV-A59 gene 4 and is not present in DPRIS. Primer C84, located in the MHV-A59 spike gene and primer C143 binding immediately upstream of the MHV-A59 S gene to a sequence which is absent in DPRIS, were then used for PCR. To detect recombinants, RNA was reverse transcribed using primer C142. PCR was performed using C147 (or C188) and C143. C188 is located upstream of C147 and was confirmed to bind specifically to the RI S gene and not to A59 by PCR (data not shown). These two primer pairs could specifically amplify recombinant cDNA.

DNA sequencing

Two recombinant-specific RT-PCR products, one from passage 4 (P4) intracellular and one from P4 virion genomic RNA, were excised from 1% agarose gel and purified by Gene clean (Bio 101 Inc., La Jolla, CA). The fragments were cloned into the *Eco*RV site of pMOSBlue-T (Amersham Life Science, Cleveland, OH) according to the manufacturer's instructions. DNA sequence analysis was performed by the dideoxynucleotide chain termination method using the T7 DNA polymerase (Pharmacia).

RESULTS

The difference in tropism between MHV-A59 and MHV-RI is most probably the result of differences in proteins responsible for attachment and entry of the host cell. The major candidate protein involved in these processes is the large surface protein S. We decided as a first step toward the production of recombinant viruses to study whether recombinant genomic RNA could be generated from coreplication of MHV-A59 and a DI RNA containing the RI S gene. The S gene sequences of MHV-A59 and MHV-RI are highly homologous, but have an important difference in one region: starting at nt 1497 (AUG = 1) the RI S gene sequence contains 156 extra nucleotides. We decided to take advantage of this difference by using it as a marker to detect recombinant MHV-A59 genomes.

Strategy for cDNA cloning

The MHV-RI spike gene, approximately 4.2 kb in length, was amplified as two overlapping PCR fragments that were cloned into a pUC-18 vector separately. These two fragments were subsequently combined to yield pMHVRIS as described under Materials and Methods. Sequence analysis of the clone confirmed that no errors had been introduced (compared with the published se-

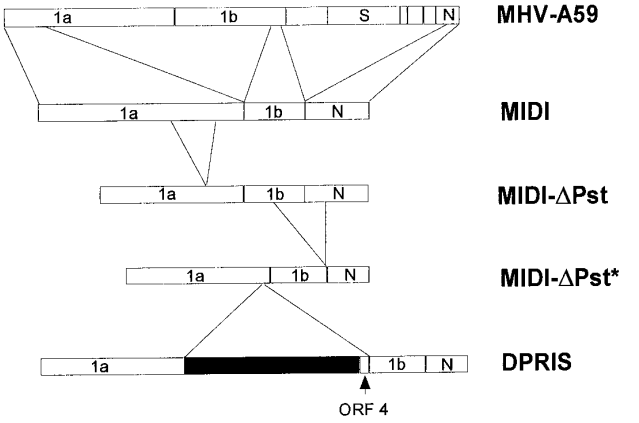

FIG. 1. Structural relationships between the different DI RNAs and MHV genomic RNA. The name of each DI RNA is indicated on the right. The black bar represents the MHV-RI S gene sequence. The MHV-A59 diagram is not drawn to scale. 1a, replicase 1a reading frame of MHV-A59; 1b, replicase 1b reading frame; S, spike ORF; N, nucleocapsid ORF.

quence in Kunita *et al.,* 1995). To obtain in frame DI constructs, a 3.9-kb fragment encompassing nt 277–4131 of the MHV-RI S gene and 120 nucleotides of the downstream gene 4 cDNA from pMHVRIS was inserted in pMIDI derivative pMIDI-ΔPst*, generating two independent clones, pDPRIS-4YL and -1L. The structure of the synthetic DI RNAs is shown schematically in Fig. 1. To confirm the full-length ORF, required for efficient DI RNA replication by MHV-A59 (De Groot *et al.,* 1992; Luytjes *et al.,* 1996), *in vitro* transcription and translation was done on these two pDPRIS constructs. Both pDPRIS-4YL and -1L encode a 190-kDa protein (data not shown).

Replicative ability of DPRIS

To study if DPRIS could be replicated in the presence of helper virus, pDPRIS-4YL and -1L were transfected into vTF7.3-infected cells, where the plasmid DNAs were transcribed into RNA by T7 polymerase and the cells were then infected with helper virus MHV-A59. Undiluted progeny virus supernatants were passaged three times. pMIDI was used as a control throughout this experiment. P3 intracellular RNA was extracted and separated in denaturing formaldehyde agarose gels and subsequently hybridized with ^{32}P-labeled probes 048 (Table 1) and C147, respectively. 048 is a 3′-end-specific probe able to detect DI, MHV genomic, and subgenomic RNAs. C147 is an MHV-RI S gene-specific probe, and therefore only hybridizes to DPRIS (data not shown). The results showed that DI DPRIS-4YL, -1L, and MIDI RNAs were replicated in the presence of MHV-A59 (Fig. 2). When 048 was used for hybridization, an extra fragment of approximately 1 kb was found in the DPRIS lane. This RNA represents a DI subgenomic RNA produced from the intergenic region between the S and ORF4a genes that was included in the fragment that was cloned from pMHVRIS. From our combined data, we concluded that DPRIS could be replicated and packaged efficiently in the presence of helper virus MHV-A59. The lower accumulation of DPRIS-4YL was not further investigated: we decided to continue our experiments with DPRIS-1L only, as it replicated most efficiently.

Development of a specific RT-PCR to screen for the recombinants

We attempted to detect recombinant genomic RNA in the intracellular RNA from cells coinfected with DPRIS and MHV-A59 and in progeny virions. For this purpose, a specific RT-PCR protocol was developed for the detection of recombinant RNA (see for oligo positions Table 1 and Fig. 5). First strand cDNA synthesis was performed using primer C142, which binds downstream of the S gene on the MHV-A59 genome, in a region not present in the DPRIS RNA. The subsequent PCR-amplification was performed using primer C147 specific for the RI S gene extra sequence and C143 which binds to the A59 genomic sequence upstream the S gene in a region not present in DPRIS (Fig. 5). We expect a 1.65-kb PCR product only when the RI S extra sequence is present in the MHV-A59 genomic RNA. As control, intracellular MHV-A59 RNA was mixed with *in vitro*-transcribed DPRIS RNA and tested by RT-PCR using the same primers. This was done to rule out the possibility that recombinants were generated by crossover during reverse transcription or PCR. A second control consisted of intracellular RNA from cells infected with MHV-A59 alone. The results for P2 and P4 RNAs showed that intracellular and virion RNAs from pDPRIS transfected, MHV-A59 infected cells yielded PCR products of the expected size (1.65 kb) (Fig. 3A). In lower passage (P0 and P1) no recombinant-specific band was detected. Both controls remained negative. A nonspecific PCR product (about 3 kb) was found in all lanes except in the A59 intracellular RNA lane. The presence of parental RNAs, DPRIS and MHV-A59, in the coinfected cells was confirmed by using primer pairs C147-C30 and C84-C143, respectively (Figs. 3B and 3C, Table 1, and Fig. 5).

To confirm the presence of recombinant RNAs and exclude RT and PCR artifacts, three P4 intracellular 1L RNA samples obtained from different infections, which were positive in the recombinant RT-PCR described above, were loaded on a denaturing low melting point agarose gel and separated by electrophoresis. Intracellular MHV-A59 RNA was used as a negative control. Genomic MHV RNA was purified from the gel and subjected to the recombinant-specific RT-PCR. C188, which binds to a region located 200 nt upstream of the extra sequence and is specific for the RI S gene, was used for RT, and C188 along with C143 for PCR (see Fig. 5). A 1.2-kb PCR product is expected for this recombinant-specific RT-PCR. Again, we were able to demonstrate the presence

TABLE 1

Oligonucleotides Used

Oligo	Sequence (5′-3′)	Polarity	Binding site in MHV-RI S	Binding site in MHV-A59	Purpose
LTK8	CAATGTAGCCTTAGGACC	−		18633–18650	PCR/Cloning
LTK51	TACTGGCTATCGATTAAC	+	2316–2333		PCR/Cloning
LTK52	AATTAGCTATCGGTCATC	−	2315–2332		PCR/Cloning
LTK53	CTAAACATGCTGTTCGTG	+	−6–12		PCR/Cloning
C142	AATGCCTAGCATACATGC	−		18681–18698	PCR
C147	ACAGCGGAGATCATAGGT	−	1631–1648		PCR/Sequencing
C143	ACGGATAGCGGTGTTAGA	+		14518–14535	PCR/Sequencing
C84	AAGGCAGGTATCATGTGA	−		16166–16181	PCR
C30	TTGCGCATACTGGTAGTC	+		3217–3234	PCR
C188	ATATTATTACACGATAGCGA	−	1105–1124		PCR
C189	TCTGACACAAACTCCAGTGG	−	1883–1902		PCR
C190	TCACCTTTGGAGCCCTTA	−	2453–2470		PCR
C191	GTTGGTTTAATAAATTATTA	−	3182–3201		PCR
C192	CATCGGACAGGTCAAGGAAT	−	3837–3856		PCR
048	GTGATTCTTCCAATTGGCCATG	−		31312–31331	Hybridization
C134	AGCTAAGATCTATATGGTACC				Linker
C133	AGCTGGTACCATATAGATCTT				Linker
C140	CGGGATCCCG				Linker

of a recombinant-specific PCR product (1.2 kb) (Fig. 4A). Significantly, the DI particle DPRIS RNA could not be detected by a DI-specific RT-PCR (Fig. 4B), whereas MHV-A59 genomic RNA was detected by a A59-specific RT-PCR (Fig. 4C). This indicated that the RNA template was free from DI RNA, excluding again the possibility of RT or PCR polymerase jumping between templates. Thus, the genomic RNAs containing the chimeric A59/RI spike gene were most likely generated from homologous recombination between the DI RNA and MHV-A59 genomic RNA. To check whether we could detect recombinants from more downstream sites of the spike gene, we designed an additional series of MHV-RI S-specific antisense primers, comprising C189, C190, C191, and C192 (Table 1 and Fig. 5), all containing at least a 2-nt mismatch with the A59 sequence at the 3′ end. These primers were used for PCR on the P2 and P4 intracellular RNA samples in which the presence of recombinant RNAs was confirmed by the recombinant-specific RT-PCR shown above (C142 for RT and C143 and C147 for PCR). C142 was used for the reverse transcription and C143 in combination with each of the antisense primers, including C188 as positive control, was used for PCR. Only the primer pair C143/C188 resulted in the amplification of a specific fragment (data not shown). This indicates that the double MHV polymerase jump occurred between nt 277 and the position of primer C189, which is nt 1883.

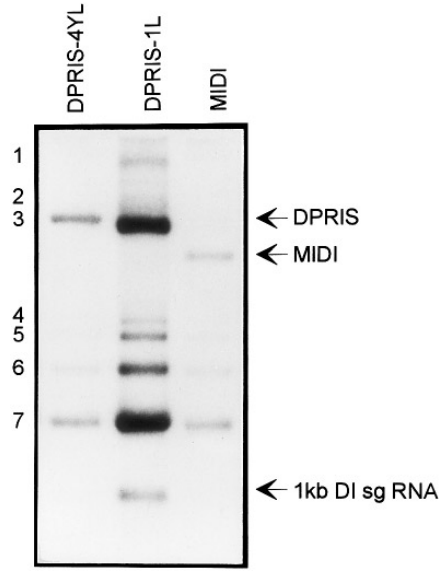

FIG. 2. Hybridization analysis of P3 intracellular RNAs. P3 intracellular RNAs isolated from L cells infected by MHV-A59 and DPRIS-4YL, -1L, or MIDI were separated on formaldehyde agarose gels and hybridized to 3′-end specific probe 048. The MHV-A59 sgRNAs are indicated by their number. RNA bands of MIDI and DPRIS are marked. A DI sgRNA band of around 1 kb in the DPRIS lanes is indicated as well.

Sequence analysis of PCR products

To find the location of the crossover sites in the recombinants, 11 plasmids of cloned recombinant-specific 1.65-kb RT-PCR products, 7 from P4 intracellular 1L RNA, and 4 from P4 virion 1L RNA were sequenced. The sequence analysis of these clones showed that they were all different, except clones 8v (virion) and 11i (intracellular). The crossovers are shown schematically in Fig. 5 and listed in Fig. 6. The examined region of homology between the RI and A59 S sequences stretches from nts 277 (the start of the RI S gene sequence in DPRIS) to 1497 (the start of the extra sequence in the RI S gene).

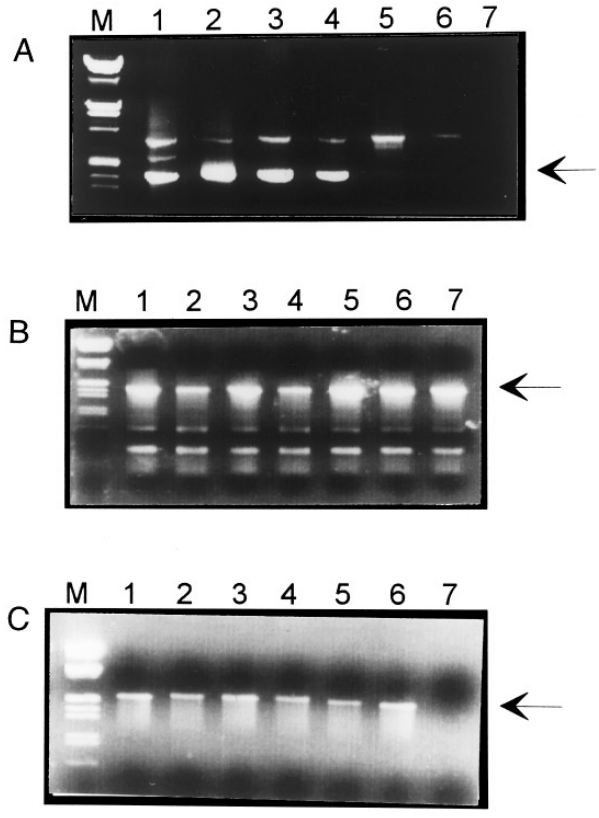

FIG. 3. Specific RT-PCRs for the detection of recombinant, DI, and MHV-A59 RNAs. RT-PCR was done on RNA isolated from P2 and P4 cell lysates and on virion RNA. Lanes M, size marker, λDNA cut with *Eco*RI and *Hin*dIII; lanes 1, P2 intracellular 1L RNA; lanes 2, P2 viral 1L RNA; lanes 3, P4 intracellular 1L RNA; lanes 4, P4 virion 1L RNA; lane 5, P4 intracellular 4YL RNA. (A) Detection of recombinant genomic RNA. Oligo C142 was used for RT and C143 and C147 for PCR (see Fig. 5 for oligo positions). C142 and C143 bind to the sequences in the ORF 4 and HE gene, respectively, which are absent in DPRIS. C147 binds to the region in the RI S gene absent in the A59 S gene. A 1.65-kb recombinant-specific PCR product (indicated by the arrow) was detected in lanes 1 to 5. The control of intracellular MHV-A59 RNA mixed with 1:10 diluted *in vitro*-synthesized DPRIS RNA gave no signal (lane 6). No specific PCR product was detected in intracellular RNA from only MHV-A59 infected cells (lane 7). An aspecific band of approximately 3 kb was found in all lanes except the MHV-A59 lane. (B) Control RT-PCR for MHV-A59. C142 was used to prime the first strand cDNA synthesis and C143 together with C84 for PCR amplication. C84 hybridizes to both the A59 and RI S genes. The specific band (1.6 kb) is indicated by the arrow. (C) Control RT-PCR for DPRIS. C147 was used for RT and C147 together with C30 for PCR. C30 hybridizes to the ORF 1a region of A59 which lies immediately upstream of the RI S gene in DPRIS. The expected 2-kb DI-specific band (arrow) appeared in all lanes except lane 7.

The 5′- and 3′-most crossovers in this region show that the minimal lengths of regions in which the polymerase has jumped were between 106–133 nt (5′-border) and 98–73 nt (3′-border). One clone (2i) contained four instead of two crossovers. The crossover back to the MHV-A59 genomic RNA was not determined, but must have occurred between nt 1653 (the end of the extra sequence) and nt 1883 (the binding site of primer C189, which is negative in RT-PCR). Crossover sites can only be determined as regions between marker mutations, but as can be seen in Fig. 6 in several cases this is only two nucleotides (clones 3v, 8v/11i, and 10v). The crossovers do not reveal any obvious role for RNA primary or secondary structure in recombination.

DISCUSSION

We are interested in the role of the spike protein in the determination of tissue tropism of MHV strains. Our approach is to attempt to convert the respiratory tropism of MHV-A59 into an enteric tropism by exchanging parts of the S gene of the respiratory strain MHV-A59 with

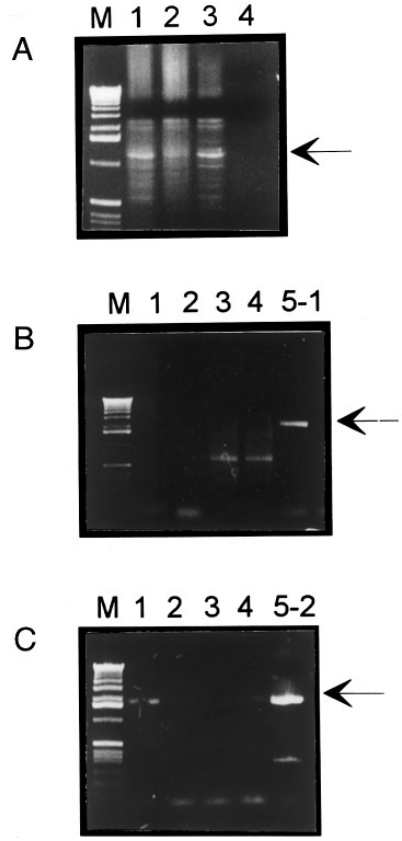

FIG. 4. RT-PCR of recombinant MHV genomic RNA isolated from low melting point agarose gel. P4 intracellular RNA from three different infections with medium containing DPRIS-1L were separated on low melting point agarose and the genome size RNA was isolated and subjected to RT-PCR. Lanes M, DNA molecular marker (BRL); lanes 1–3, three different samples of P4 genomic RNA; lanes 4, P4 intracellular MHV-A59 RNA; lane 5-1, pDPRIS DNA; lane 5-2, P4 intracellular MHV-A59 RNA unpurified. The positions of the specific RT-PCR products are indicated by arrows. (A) Recombinant-specific RT-PCR on LMP-purified 1L genomic RNA. C142 was used for RT, C188, and C143 for PCR. C188 can only bind to MHV-RI S gene and not to the MHV-A59 S gene (see Fig. 5). A 1.2-kb-specific band is detected. (B) Control RT-PCR for DPRIS using the same set of oligonucleotides as described in the legend of Fig. 3C. (C) Control RT-PCR for MHV-A59 intracellular RNA using the same set of oligonucleotides as described in the legend of Fig. 3B.

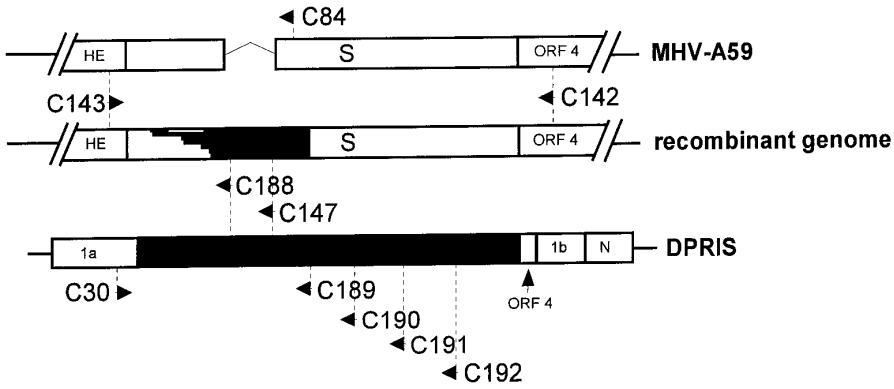

FIG. 5. Schematic representation of the primer positions and recombinant RNAs. Oligonucleotide primers are indicated by arrows and names (see Table 1); the dotted lines show their binding sites. The black bars represent the MHV-RI S sequence, the white bars the MHV-A59 sequence. The intermediate diagram represents the 5′-crossover sites of 11 recombinants. The 3′-crossover sites are not determined, but do not extend beyond the position op primer C189. The gap region in MHV-A59 S is indicated.

corresponding parts of the genome of the enterotropic strain MHV-RI and study the properties of the recombinant virus.

For smaller RNA viruses such as alphaviruses and picornaviruses mutagenesis of their genomes is possible because full-length infectious cDNA clones have been constructed. This has profoundly advanced the study of viral replication and pathogenesis (Hahn *et al.,* 1989a; 1989b; Lustig *et al.,* 1988; Kohara *et al.,* 1985; La Monica *et al.,* 1986; Omata *et al.,* 1986; Pincus *et al.,* 1986). However, for MHV, the extreme length of the genome poses an obvious technical problem. The only possibility to mutagenize site-specifically the MHV genome is currently by using homologous RNA recombination and several successful attempts have been reported (Koetzner *et al.,* 1992; Masters *et al.,* 1994; Van der Most *et al.,* 1992).

The most efficient approach uses DI particles as the source of donor RNA (Masters *et al.,* 1994; Van der Most *et al.,* 1992). The advantage of a replicating DI is that the amount of DI RNA increases during replication and, more importantly, during passaging, which increases the chance of recombination between DI RNA and genomic RNA. Some investigators even observed that the increased rate of recombination between replicating DI RNA and helper virus RNA was high enough to identify recombinants without the necessity for selection directly (Masters *et al.,* 1994). However, very significantly, the DI system in all the published reports was limited in that it only allowed the introduction of mutations into the very 3′ and 5′ end of the MHV genome. The donor RNA contained these terminal sequences of MHV, as they are required for replication, thus only one crossover event was necessary to generate a viable mutant. We decided to set up a similar protocol, based on replicating DI RNA, to mutagenize internal regions on the MHV genome. However, this approach would rely on double crossover events, i.e., from the acceptor genomic RNA to the donor DI RNA and back.

We show first that after cloning a 3.9-kb fragment of the MHV-RI S gene cDNA into the MIDI derivative, MIDI-ΔPst*, the resulting DI construct DPRIS RNA could be replicated and passaged efficiently in MHV-A59-infected cells. The spike gene in DPRIS is discontinuously fused to the terminal sequences from the MHV genome required for replication of the DI RNA. Therefore, double homologous recombination events are required for the introduction of a mutation into the genomic A59 S gene. It is generally accepted that RNA recombination in coronaviruses occurs by a copy-choice mechanism in which the polymerase jumps between templates, as was first proposed by Kirkegaard and Baltimore (1986). Thus to mutate the genomic S gene, first an homologous jump from the genomic RNA template to the synthetic DI RNA template must occur and then jumping back again to the genomic RNA, either during negative or positive strand RNA synthesis. We show in this report that in the absence of positive selection pressure, recombination between DPRIS and the MHV genomic RNA could be detected, but only by a highly specific and sensitive RT-PCR. This was not surprising, since it has been described that less than 10% of the total virus progeny contained a single crossover when copassaging a DI particle with a helper virus without selection pressure (Masters *et al.,* 1994). The frequency of double crossover recombinations is expected to be much lower. Recombinant genomic RNA was present in the pool of intracellular RNAs as shown by specific RT-PCR. More convincingly, recombinant RNA could be detected in purified virions with specific RT-PCR. Finally, MHV genomic RNA purified from DI by using low melting point agarose gel also yielded a recombinant-specific PCR signal. All the data strongly suggest that homologous recombination between synthetic DI RNA and MHV-A59 genomic RNA truly takes place.

In low passage (P0 and P1) no recombinant-specific RT-PCR products were detected in intracellular and virion

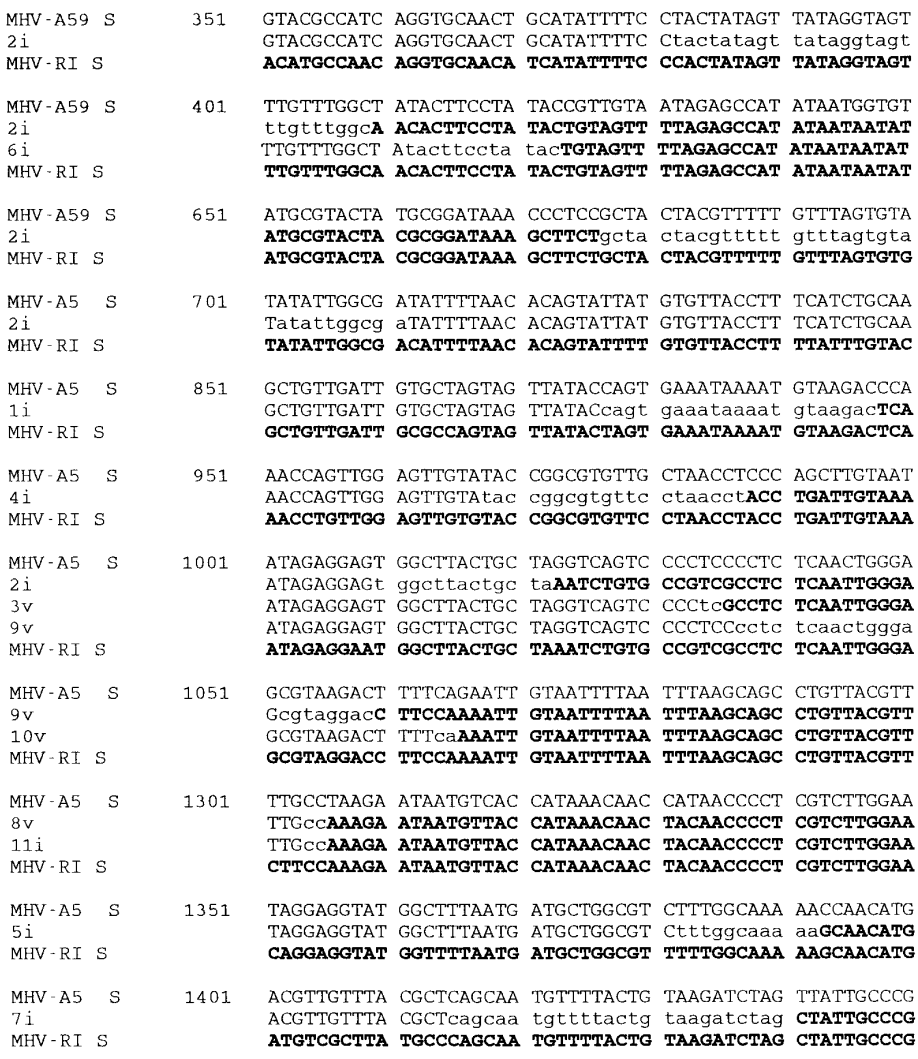

FIG. 6. Alignment of the crossover region sequences of the recombinant-specific RT-PCR clones and the MHV-A59 and MHV-RI S genes (Luytjes *et al.,* 1987; Kunita *et al.,* 1995). The recombinant sequence is shown between the MHV-A59 sequence (top, regular print) and the MHV-RI sequence (bottom, bold print). The region in which the crossover must have occurred, defined by the flanking sequence differences between the MHV-A59 and -RI S genes is indicated in lowercase. Numbers represent the position relative to the start of the MHV-A59 S gene sequence.

RNA. Probably, the levels of DI RNA in these cells were too low to support recombination.

Sequence analysis of 11 independently cloned PCR products showed that there are different species of recombinant RNAs, with crossover sites unevenly distributed over the examined 1.65-kb region of the S gene. The sample size is too small to allow the conclusion that this distribution is random or nonrandom in this area. However, since we have not been able to detect recombination events downstream of nt 1883, recombination does seem to be nonrandom when the entire S gene is considered. In earlier studies of RNA recombination between related MHV strains, crossovers were randomly distributed when studied directly, but after selection at the protein level by virus passaging, became clustered in regions in which amino acid changes were tolerated (Banner *et al.,* 1990; Banner and Lai, 1991). Such a region was observed in the S1 part of the spike gene. Interestingly, the crossovers that we report are all in this region, suggesting that selection did take place. If crossovers downstream of the extra sequence are selected against, such a selection would most likely occur at the protein level, i.e., by the properties of the S protein on the recombinant virus particle. MHV-RI virus grows slowly and to low titers in susceptible cells. Conceivably, the RI S protein plays a role in slow replication, for instance by slow maturation. Certain recombinant viruses, containing S proteins that had acquired those parts of the RI S protein that cause the delayed replication phenotype, would then have a selective disadvantage.

All recombinants represent precise jumps, without insertions or deletions. When we define the crossover region as the region of identity between nonmatching nucleotides, most polymerase jumps occurred in stretches

of at least 9 nt. However, interestingly, in three cases the crossover site could be pinpointed to as little as two nucleotides. It has been hypothesized that in polymerase jumping the free nascent RNA chain helps to realign the polymerase complex to the acceptor RNA, by annealing (Jarvis and Kirkegaard, 1992; Nagy and Bujarsky, 1995) or by heteroduplex formation (Romanova *et al.,* 1986; Tolskaya *et al.,* 1987). Even when one of the 2-nt crossover sites is dismissed (10v) after allowing for G-U base pairing, two alignment events would have had to occur on only two nucleotides. This may be too short to explain the precise recombination we observe. Therefore, the alternative model in which the replicase/RNA complex realigns as a whole seems more attractive. The docking of the complex in this model is guided by the recognition of local RNA structure, which is not very different between the two strands.

Several factors can play a role in determining recombination sites at the donor RNA level and have been studied mostly for RNA viruses. First, in many cases the presence of local secondary structure has been suggested to invoke the polymerase to pause and detach (Carpenter *et al.,* 1995). A prediction of secondary structure of A59 and RI S RNA did not reveal any clear correlation with crossover sites in the recombinants. Also, repeats of nucleotides, specifically A and U, have been suggested to be involved in template switching by causing polymerase pausing (Nagy and Bujarsky, 1996). In these cases, however, recombination was often imprecise because of misalignment. We do not observe such a phenomenom in the recombinants. We thus cannot conclusively determine if any of these factors are at play in the generation of the recombinant genomic RNA.

This is the first report of an introduction of mutations derived from coreplicating synthetic DI-RNA into an internal region of the MHV genomic RNA. Although potentially powerful, this approach can only be useful when recombinant virus particles can be isolated. One way to achieve this is to apply a selective pressure procedure that enriches for recombinant viruses in the progeny. We are currently establishing such a system.

ACKNOWLEDGMENTS

We thank Robbert van der Most, Caroline Brown, Evelyne Bos, Kurt Tobler, and Mathias Ackermann for stimulating discussions. This work was supported by Grant 31-39′728.93 of the Swiss Science Foundation and a grant from the Swiss Academy of Medical Sciences.

REFERENCES

Banner, L. R., Keck, J. G., and Lai, M. M. C. (1990). A clustering of RNA recombination sites adjacent to a hypervariable region of the peplomer gene of murine coronavirus. *Virology* 175, 548–555.

Banner, L. R., and Lai, M. M. C. (1991). Random nature of coronavirus RNA recombination in the absence of selection pressure. *Virology* 185, 441–445.

Barthold, S. W. (1986). Mouse hepatitis virus biology and epizootiology. *In* "Viral and Mycoplasmal Infections of Laboratory Rodents" (P. N. Bhatt and R. O. Jacoby, Eds.), pp. 571–601. Academic Press, New York.

Barthold, S. W. (1987). Host age and genotypic effects on enterotropic mouse hepatitis virus infection. *Lab. Anim. Sci.* 37, 36–40.

Barthold, S. W., Beck, D. S., and Smith, A. L. (1993). Enterotropic coronavirus (mouse hepatitis virus) in mice: influence of host age and strain on infection and disease. *Lab. Anim. Sci.* 43, 276–284.

Barthold, S. W., Smith, A. L., and Povar, M. L. (1985). Enterotropic mouse hepatitis virus infection in nude mice. *Lab. Anim. Sci.* 35, 613–618.

Carpenter, C. D., Oh, J-W., Zhang, C., and Simon, A. E. (1995). Involvement of a stem-loop structure in the location of junction sites in viral RNA recombination. *J. Mol. Biol.* 245, 608–622.

Collins, A. R., Knobler, R. L., Powell, H., and Buchmeier, M. J. (1982). Monoclonal antibodies to murine hepatitis virus-4 (strain JHM) define the viral glycoprotein responsible for attachment and cell-cell fusion. *Virology* 119, 358–.

Compton, S. R., Barthold, S. W., and Smith, A. L. (1993). The cellular and molecular pathogenesis of coronaviruses. *Lab. Anim. Sci.* 43, 15–28.

De Groot, R. J., Van der Most, R. G., and Spaan, W. J. M. (1992). The fitness of defective interfering murine coronavirus DI-a and its derivatives is decreased by nonsense and frameshift mutations. *J. Virol.* 66, 5898–5905.

Dalziel, R. G., Lampert, P. W., Talbot, P. J., and Buchmeier, M. J. (1986). Site-specific alteration of murine hepatitis virus type 4 peplomer glycoprotein E2 results in reduced neurovirulence. *J. Virol.* 59, 463–471.

Daniel, C., and Talbot, P. J. (1990). Protection of mice from lethal coronavirus MHV-A59 infection by monoclonal affinity-purified spike glycoprotein. *In* "Coronaviruses and Their Diseases" (D. Cavanagh and T. D. K. Brown, Eds.), pp. 205–210. Plenum Press, New York.

Fazakerley, J. K., Parker, S. E., Bloom, F., and Buchmeier, M. J. (1992). The V5A13.1. envelope glycoprotein deletion mutant of mouse hepatitis virus type-4 is neuroattenuated by its reduced rate of spread in the central nervous system. *Virology* 187, 178–188.

Fleming, J. O., Trousdale, M. D., El-Zaatari, F. A. K., Stohlman, S. A., and Weiner, L. A. (1986). Pathogenicity of antigenic variants of murine coronavirus JHM selected with monoclonal antibodies. *J. Virol.* 58, 869–875.

Hahn, Y. S., Grakoui, A., Rice, C. M., Strauss, E. G., and Strauss, J. H. (1989a). Mapping of RNA-temperature-sensitive mutants of Sindbis virus: complementation group F mutants have lesions in nsP4. *J. Virol.* 63, 1194–1202.

Hahn, Y. S., Strauss, E. G., and Strauss, J. H. (1989b). Mapping of RNA-temperature-sensitive mutants of Sindbis virus: assignment of complementation groups A, B, and G to nonstructural proteins. *J. Virol.* 63, 3142–50.

Hasony, H. J., and Macnaughton, M. R. (1981). Antigenicity of mouse hepatitis virus strain 3 subcomponents in C57 strain mice. *Arch. Virol.* 69, 33–.

Hingley, S. T., Gombold, J. L., Lavi, E., and Weiss, S. R. (1994). MHV-A59 fusion mutants are attenuated and display altered hepatotropism. *Virology* 200, 1–10.

Jarvis, T. C., and Kirkegaard, K. (1991). The polymerase in its labyrinth: mechanisms and implications of RNA recombination. *Trends Genet.* 7, 186–191.

Keck, J. G., Soe, L. H., Markino, S., and Lai, M. M. C. (1988). RNA recombination of murine coronavirus: recombination between fusion-positive mouse hepatitis virus A59 and fusion-negative mouse hepatitis virus. *J. Virol.* 62, 1989–1998.

Keck, J. G., Stohlman, S. A., Soe, L. H., Makino, S., and Lai, M. M. C. (1987). Multiple recombination sites at the 5′-end of murine coronavirus RNA. *Virology* 156, 331–341.

Kirkegaard, K., and Baltimore, D. (1986). The mechanism of RNA recombination in poliovirus. *Cell* 47, 433–443.

Koetzner, C. A., Parker, M. M., Richard, C. S., Sturman, L. S., and Masters, P. S. (1992). Repair and mutagenesis of the genome of a deletion

mutant of the coronavirus mouse hepatitis virus by targeted RNA recombination. *J. Virol.* 66, 1841–1848.

Kohara, M., Omata, T., Kameda, A., Semler, B. L., Itoh, H., Wimmer, E., and Nomoto, A. (1985). In vitro phenotypic markers of a poliovirus recombinant constructed from infectious cDNA clones of the neurovirulent Mahoney strain and the attenuated sabin strain. *J. Virol.* 53, 786–792.

Kunita, S., Zhang, L., Homberger, F. R., and Compton, S. R. (1995). Molecular characterization of the S proteins of two enterotropic murine coronavirus strains. *Virus Res.* 35, 277–289.

Lai, M. M. C., Baric, R. S., Makino, S., Keck, J. G., Egbert, J., Leibowitz, J. L., and Stohlman, S. A. (1985). Recombination between nonsegmented RNA genomes of murine coronavirus. *J. Virol.* 56, 449–456.

La Monica, N., Meriam, C., and Racaniello, V. C. (1986). Mapping of sequences required for mouse neurovirulence of poliovirus type 28 Lansing. *J. Virol.* 57, 515–525.

Langridge, L., Langridge, P., and Bergquist, P. L. (1980). Extraction of nucleic acids from agarose gels. *Anal. Biochem.* 103, 661–670.

Lustig, S., Jackson, A. C., Hahn, C. S., Griffin, D. E., Strauss, E. G., and Strauss, J. H. (1988). Molecular basis of Sindbis virus neurovirulence in mice. *J. Virol.* 62, 2329–2336.

Luytjes, W., Sturman, L. S., Bredenbeek, P. J., Charité, J., Van der Zeijst, B. A. M., Horzinek, M. C., and Spaan, W. J. M. (1987). Primary structure of the glycoprotein E2 of coronavirus MHV-A59 and identification of the trypsin cleavage site. *Virology* 161, 479–487.

Luytjes, W., Gerritsma, H., and Spaan, W. J. M. (1996). Replication of synthetic defective interfering RNAs derived from coronavirus mouse hepatitis virus-A59. *Virology* 216, 174–183.

Makino, S., Fleming, J. O., Keck, J. G., Stohlman, S. A., and Lai, M. M. C. (1987). RNA recombination of coronavirus: location of neutralizing epitopes and neuropathogenic determinants on the carboxyl terminus of peplomers. *Proc. Natl. Acad. Sci. USA* 84, 6567–6571.

Makino, S., Keck, J. G., Stohlman, S. A., and Lai, M. M. C. (1986). High-frequency RNA recombination of murine coronaviruses. *J. Virol.* 57, 729–737.

Makino, S., Taguchi, F., and Fujiwara, K. (1984). Defective interfering particles of mouse hepatitis virus. *Virology* 133, 9–17.

Masters, P. S., Koetzner, C. A., Kerr, C. A., and Heo, Y. (1994). Optimization of targeted RNA recombination and mapping of a novel nucleocapsid gene mutation in the coronavirus mouse hepatitis virus. *J. Virol.* 68, 328–337.

Meinkoth, J., and Wahl, G. (1984). Hybridization of nucleic acids immobilized on solid supports. *Anal. Biochem.* 138, 267–284.

Nagy, P. D., and Bujarsky, J. J. (1995). Efficient system of homologous RNA recombination in brome mosaic virus: sequence and structure requirements and accuracy of crossovers. *J. Virol.* 69, 2547–2556.

Nagy, P. D., and Bujarsky, J. J. (1996). Homologous RNA recombination in brome mosaic virus: AU-rich sequences decrease the accuracy of crossovers. *J. Virol.* 70, 415–426.

Omata, T., Kohara, M., Kuge, S., Komatsu, T., Abe, S., Semler, B. L., Kameda, A., Itoh, H., Arita, M., Wimmer, E., and Nomoto, A. (1986). Genetic analysis of the attenuation phenotype of poliovirus type 1. *J. Virol.* 58, 348–358.

Peng, D., Koetzner, C. A., Masters, P. S. (1995). Analysis of second-site revertants of a murine coronavirus nucleocapsid protein deletion mutant and construction of nucleocapsid protein mutants by targeted RNA recombination. *J. Virol.* 69, 3449–3457.

Pincus, S. E., and Wimmer, E. (1986). Production of guanidine-resistant and dependent poliovirus mutants from cloned cDNA mutations in polypeptide 2c are directly responsible for altered guanidine sensitivity. *J. Virol.* 60, 793–796.

Romanova, L. I., Blinov, V. M., Tolskaya, E. A., Viktorova, E. G., Kolesnikova, M. S., Guseva, E. A., and Agol, V. I. (1986). The primary structure of crossover regions of intertypic poliovirus recombinants: a model of recombination between RNA genomes. *Virology* 155, 202–213.

Sambrook, J., Fritsch, E. F., and Maniatis, T. (1989). "Molecular Cloning." Cold Spring Harbor Laboratory Press, Cold Spring Harbor, NY.

Spaan, W. J. M., Rottier, P. J. M., Horzinek, M. C., and Van der Zeijst, B. A. M. (1981). Isolation and identification of virus-specific mRNAs in cells infected with mouse hepatitis virus (MHV-A59). *Virology* 108, 424–434.

Tolskaya, E. A., Romanova, L. I., Blinov, V. M., Viktorova, E. G., Sinyakov, A. N., Koleskinova, M. S., and Agol, V. I. (1987). Studies on the recombination between RNA genomes of poliovirus: the primary structure and nonrandom distribution of crossover regions in the genomes of intertypic poliovirus recombinants. *Virology* 161, 54–61.

Van der Most, R. G., Bredenbeek, P. J., and Spaan, W. J. M. (1991). A domain at the 3′ end of the polymerase gene is essential for encapsidation of coronavirus defective interfering RNAs. *J. Virol.* 65, 3219–3226.

Van der Most, R. G., Heijnen, L., Spaan, W. J. M., and De Groot, R. J. (1992). Homologous RNA recombination allows efficient introduction of site-specific mutations into the genome of coronavirus MHV-A59 via synthetic co-replicating RNAs. *Nucleic Acids Res.* 13, 3375–3381.

Van der Most, R. G., Rutjes, S., and Spaan, W. J. M. (1995). Translation but not the encoded sequence is essential for the propagation of the defective interfering RNAs of the coronavirus mouse hepatitis virus. *J. Virol.* 69, 3744–3751.

Wege, H., Winter, J., and Meyermann, R. (1988). The peplomer protein E2 of coronavirus JHM as a determinant of neurovirulence: definition of critical epitopes by variant analysis. *J. Gen. Virol.* 69, 87–98.